Available online at www.sciencedirect.com
SCIENCE DIRECT®
Bioorganic & Medicinal Chemistry 13 (2005) 1325–1332
Bioorganic & Medicinal Chemistry

Formylchromone derivatives as irreversible and selective inhibitors of human protein tyrosine phosphatase 1B. Kinetic and modeling studies

Yi Sup Shim, Ki Chul Kim, Kyung A. Lee, Suja Shrestha, Keun-Hyeung Lee, Chan Kyung Kim and Hyeongjin Cho*

Department of Chemistry and Institute of Molecular Cell Biology, Inha University, Yonghyun-dong, Nam-ku, Incheon 402-751, Republic of Korea

Received 15 October 2004; revised 5 November 2004; accepted 5 November 2004
Available online 25 November 2004

Abstract—A series of formylchromone derivatives were synthesized as PTP1B inhibitors and some of them were potent against PTP1B with IC_{50} values as low as 1.0 μM. They exhibited remarkable selectivity for PTP1B over other human PTPases. Kinetic studies revealed that formylchromone derivatives are irreversible and active site-directed inhibitors. Molecular modeling study identified the orientation of the inhibitor bound at the active site of PTP1B.

1. Introduction

The activities and functions of cellular proteins are often regulated by posttranslational modifications. Tyrosine phosphorylation is an example of those modifications and the reversible nature of the phosphorylation provides the basis for the communication between the signaling proteins inside cell.[1–4] The phosphorylation state of a protein is dynamically controlled by the action of protein tyrosine kinases (PTKs) and protein tyrosine phosphatases (PTPases); PTKs catalyze the tyrosine phosphorylation and PTPases catalyze the reverse reaction.[5,6] While the importance of PTKs in cellular events has been recognized for many decades, PTPases have relatively short history of investigation. PTPase was first identified in 1988 by isolation of PTP1B in homogeneity from human placenta.[7] Despite the late start, significant progresses have been achieved in PTPase study and these enzymes are now appreciated as important regulators for the homeostasis of cell.[2–4] Aberrant action of PTPases is often linked to cellular dysfunction and implicated in a diverse of diseases including diabetes, obesity, autoimmune diseases, infectious diseases, inflammation, cancer, osteoporosis, and neurodegeneration.[8–10] Inhibitors of PTPases, therefore, could be potential drugs against those diseases. Among those, type 2 diabetes and obesity are believed to be associated with the defect in insulin receptor signaling and the fault, supposedly, could be recovered by the inhibition of a certain PTPase(s) and consequential prolonged phosphorylation of the insulin receptor kinase.[11–14] PTP1B is considered as one of the most likely targets among PTPase family.[11–14]

A variety of inhibitors of PTPases has been designed and reported in the literature. Many of those incorporated phosphate-mimicking functionalities such as $-CH_2PO_4^{2-}$, $-CF_2PO_4^{2-}$, $-COCO_2^-$, or CO_2^- to list a few.[5,15,16] Some of them have proven difficult to achieve cell permeability especially when the inhibitors have multiple acidic functional groups. Simulation of phosphate functionality and evasion of multiple negative charges have often been incompatible with each other and this contradiction posed a hurdle in the development of cell active PTPase inhibitors. Prodrug approach might be one way to circumvent the obstacle and the pharmacophores without charge were also precedented.[17–23]

During the course of our search for PTPase inhibitors, we found that 3-formylchromone (**TP01**, 4-oxo-4*H*-1-benzopyran-3-carboxaldehyde) and its derivatives

Keywords: Protein tyrosine phosphatase; Irreversible inhibitor; Formylchromone; Enzyme kinetics.
* Corresponding author. Tel.: +82 32 860 7683; fax: +82 32 867 5604; e-mail: hcho@inha.ac.kr

0968-0896/$ - see front matter © 2005 Elsevier Ltd. All rights reserved.
doi:10.1016/j.bmc.2004.11.006

behave as inhibitors of PTPases and reported the initial results recently.[15] To take the advantage that 3-formylchromone moiety can serve as a neutral pharmacophore for PTPase inhibitor design, we performed intensive derivatization of 3-formylchromone and evaluated the inhibitory potency of the derivatives. Kinetic and molecular modeling studies were also performed to study the structural features of the inhibitor binding to PTP1B.

2. Results and discussion

2.1. Structure–inhibitory activity relationship of formylchromone derivatives

A series of formylchromone derivatives were chemically synthesized and evaluated for their inhibitory activity against human PTPases with *p*-nitrophenyl phosphate (*p*NPP) as a substrate (Fig. 1). Initially, inhibitory potency of the compounds was measured against PTP1B and the result was expressed as the concentration of the compound, which inhibited PTP1B activity by 50% (IC_{50}) (Table 1). The enzyme and inhibitor were preincubated for 10 min before initiation of the enzyme reaction by addition of the substrate. Initial enzyme assay proved that most of the formylchromone derivatives behaved as inhibitors of the PTPases and several of them exhibited IC_{50} values approaching nanomolar concentration comparable to those of the most successful inhibitors previously developed. Even though PTP1B inhibitors with lower IC_{50} values were precendented, some of them were peptides with high molecular weight. Furthermore, most of the small molecular weight inhibitors with nanomolar IC_{50} values were assayed using phosphotyrosyl(pTyr)-peptide as a substrate. At least to certain classes of inhibitors, pTyr-peptide phosphatase assay is known to give lower IC_{50} values compared to the *p*NPP assay adopted in this study.[20] Therefore, the IC_{50} values of the formylchromone derivatives cannot be directly compared with those of the PTP1B inhibitors obtained from pTyr-peptide phosphatase assay.

Table 1. Inhibition of PTP1B by formylchromone derivatives[a]

Compound	IC_{50} (μM)
TP01[b]	73 ± 2
TP07[b]	20 ± 1
TP13	7.1 ± 0.5
TP14	2.5 ± 0.4
TP15	11 ± 2
TP16	9.7 ± 0.5
TP17	11 ± 1
TP18	16 ± 3
TP19	7.7 ± 0.4
TP20	8.2 ± 1.7
TP21	7.6 ± 0.3
TP22	10 ± 0.1
TP23	6.2 ± 0.2
TP24	7.8 ± 0.6
TP25	6.0 ± 0.6
TP26	6.0[c]
TP27	3.2 ± 0.8
TP28	16 ± 2
TP29[b]	14 ± 3
TP30	3.3 ± 0.3
TP31[b]	4.3 ± 0.1
TP32	2.0 ± 0.1
TP33	1.1 ± 0.3
TP34	1.0 ± 0.2
TP35	36 ± 6
TP36	18 ± 5
TP37	13 ± 2

[a] The IC_{50} values reported were calculated from at least two independent experiments.
[b] These compounds were reported previously (15).
[c] Estimated from the IC_{50} value obtained with a mixture of **TP25** and **TP26**.

Even though lowering IC_{50} value of enzyme inhibitors is the merit for medicinal chemists, there are many other aspects to be considered for the drug development. A previously described oxazole azolidinedione derivative which exhibited quite high IC_{50} of 50 μM in *p*-nitrophenyl phosphatase assay and 1.9 μM in pTyr-peptide phosphatase assay lowered plasma glucose level effectively in mouse experiment[20] indicating that the lower IC_{50} is not always the most important factor. Equally important thing to be considered is cell permeability and, in this respect, neutral or modestly charged inhibitors are better suited as a drug candidate. Formylchromone moiety provides a neutral pharmacophore and has the advantage in this regard. For example, **TP34** has been proved to be an effective PTPase inhibitor in intact cell and, at 2 μM concentration in culture medium, the inhibitory effect was comparable with those obtained with 20 μM orthovanadate or 1 μM phenylarsine oxide in prevention of apoptosis.[24]

Selected compounds which exhibited $IC_{50} < 3.3$ μM against PTP1B were further evaluated for their inhibitory activity against other human PTPases; membrane proximal catalytic domain of LAR (LAR-D1), TC-PTP, and catalytic domain of SHP-1. As shown in Table 2, selectivity of these compounds for PTP1B was remarkable against LAR-D1 and medium to high against TC-PTP and SHP-1. Among them, **TP33** and **TP34** were PTP1B-selective with IC_{50} values 500-, 30-, and >10-fold lower compared to those against LAR-D1, TC-PTP and SHP-1 respectively. Noteworthy is the 30-fold selectivity against TC-PTP, the most homologous PTPase to PTP1B. Because of the multiplicity of PTPases in human, targeting a PTPase for drug development imposes a challenging hurdle of selective inhibition of a single PTPase. In this regard, the selectivity observed with formylchromone derivatives is promising.

2.2. Formylchromone derivatives are irreversible and active site-directed inhibitors of PTPases

To study the nature of the inhibition by formylchromone derivatives, kinetic experiments were performed. When the hydrolysis of *p*NPP by PTP1B was monitored continuously in the presence and absence of inhibitor, time-dependent decrease of the enzyme activity followed by steady-state reaction rate characteristic for slow-binding or irreversible inhibition was observed (Fig. 2). To distinguish the mode of inhibition between these

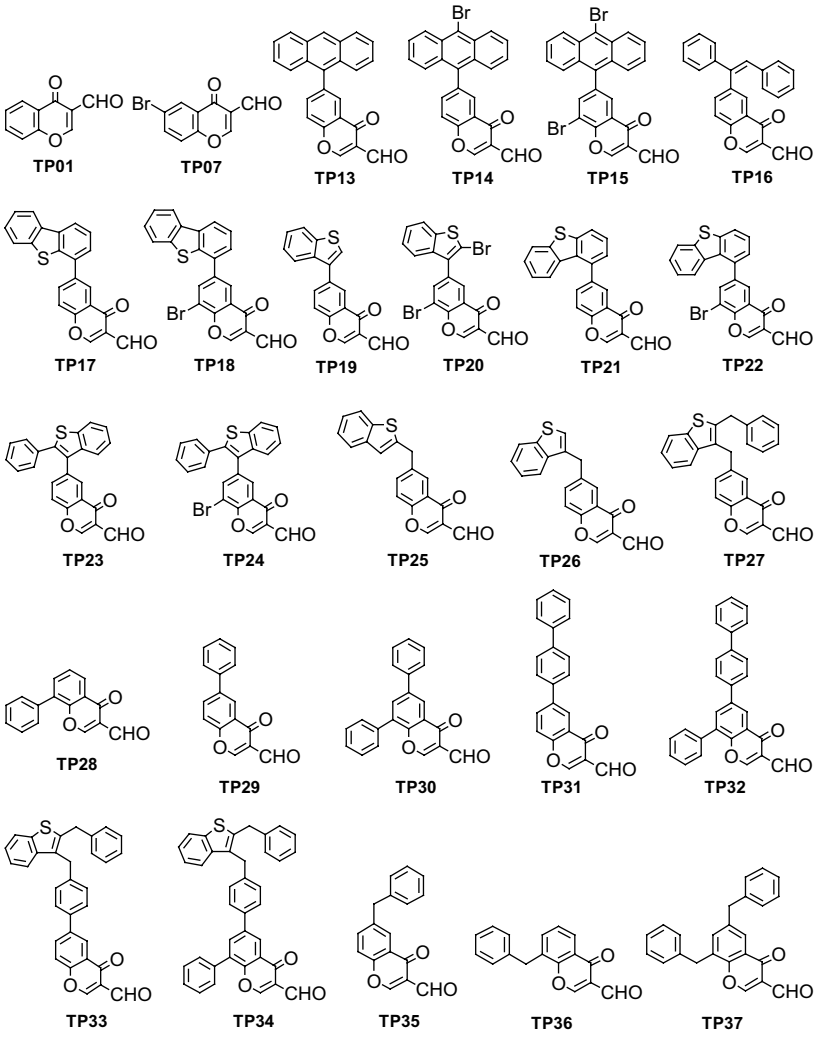

Figure 1. Structures of formylchromone derivatives used in this study.

Table 2. Inhibition of PTPases by selected compounds

Compound	IC_{50} (μM)			
	PTP1B	LAR-D1	TC-PTP	SHP-1cat
TP14	2.5 ± 0.4	570 ± 130	34 ± 2	5.7 ± 1.4
TP27	3.2 ± 0.8	>1000	48 ± 10	6.2 ± 1.1
TP30	3.3 ± 0.3	>1000	54 ± 7	8.2 ± 0.9
TP32	2.0 ± 0.1	>1000	55 ± 2	6.5 ± 1.2
TP33	1.1 ± 0.3	>1000	32 ± 3	15 ± 2.2
TP34	1.0 ± 0.2	520 ± 80	34 ± 6	14 ± 2

two possibilities, PTP1B was preincubated for 20 min with or without **TP07** and then diluted 50-fold into the assay mixture containing substrate. In the absence of the inhibitor, the reaction progress was linear over the examined assay period, while in the presence of the inhibitor, the PTPase activity was not recovered to a measurable extent up to 30 min after dilution indicating that **TP07** is a irreversible inhibitor of PTP1B (Fig. 3A). The inhibitor concentration was 200 μM before dilution and 4 μM after dilution. Considering that IC_{50} of **TP07** for PTP1B was 20 μM, if the **TP07** inhibition of PTP1B

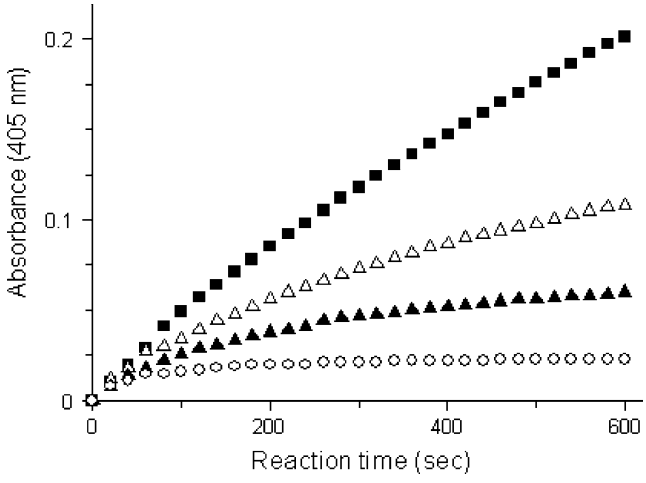

Figure 2. Progresses of *p*NPP hydrolysis by PTP1B in the absence and presence of **TP07**. PTP1B was added at 37 °C into a cuvette containing *p*NPP and inhibitor in buffer A and the reaction was continuously monitored at 405 nm by a spectrophotometer equipped with a thermostatic cell holder. Inhibitor concentrations were 0 μM (■), 50 μM (△), 100 μM (▲) and 300 μM (○).

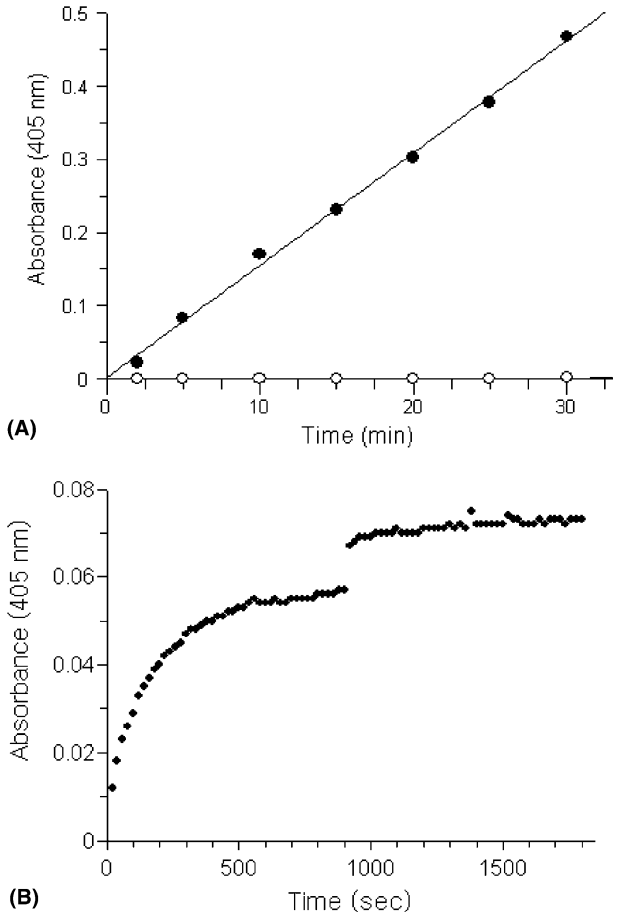

Figure 3. Irreversible inhibition of PTP1B by **TP07**. (A) PTP1B was preincubated for 20 min at 25 °C in the absence (●) or presence (○) of 200 μM **TP07**. Subsequently, the inhibited enzyme mixture was diluted 50-fold into the assay mixture. At the indicated time points, aliquots of the mixture was removed and quenched with 0.5 M NaOH solution to measure the absorbance at 405 nm. Similar result was obtained in a separate experiment using 50 μM **TP27**. (B) Enzyme reaction was initiated by addition of PTP1B into a cuvette containing 0.1 mM *p*NPP and 300 μM **TP07** in buffer A and the absorbances were recorded. At 900 s, 10-fold excess *p*NPP was added to the reaction mixture. Sudden jump of the absorbance is due to the *p*-nitrophenolate contaminated in *p*NPP.

is reversible, significant PTPase activity should be observed in the presence of 4 μM of **TP07**. The irreversible nature of the inhibition was further supported by another experiment. PTPase reaction was started in the presence of **TP07** and, when the enzyme was completely inhibited, 10-fold excess of *p*NPP was added to the assay mixture. The inhibition of PTP1B by **TP07** was not reversed by addition of excess substrate (Fig. 3B) providing another evidence for the irreversible nature of the inhibition.

Binding of the formylchromone derivatives at the active site of PTP1B was demonstrated by the observation that the enzyme inactivation was prevented by inorganic phosphate, a weak active site-directed inhibitor of PTPases. When PTP1B was preincubated with **TP07** in the absence of inorganic phosphate, time-dependent decrease of enzyme activity was observed (Fig. 4A). On the other hand, when the enzyme was incubated with **TP07** in the presence of increasing amounts of phosphate, protective effect of PO_4^{2-} against the enzyme inactivation was observed (Fig. 4B–D). Only little enzyme inactivation was observed in the presence of 100 mM phosphate (Fig. 4D).

To study the kinetics of inactivation, PTP1B was preincubated with **TP07** in the absence of substrate for different time periods and the remaining PTPase activities were measured. Semilogarithmic plots of the remaining enzyme activity versus preincubation time were linear over the examined periods (Fig. 5A), indicating that the kinetics of this inactivation is pseudo-first order. Apparent first-order inactivation rate constants (k_{app}) were calculated from the slopes of the lines. The rate of inactivation was found to be dependent on the inhibitor concentration, since the rate of inactivation increases with increasing amounts of inhibitor over a concentration range of 40–400 μM. The plot of the inactivation rate versus inhibitor concentration exhibited saturation kinetics (Fig. 5B) indicating that the enzyme forms a Michaelis-type complex with inhibitor prior to the covalent enzyme–inhibitor complex formation.

$$E + I \rightleftharpoons E \cdot I \rightarrow E - I$$

In the presence of excess inhibitor, the apparent inactivation rate constant, k_{app}, is given by

$$k_{app} = k_{inact}[I]/(K_i + [I])$$

where K_i is the dissociation constant (equilibrium binding constant) for the Michaelis complex formation and k_{inact} is the rate constant for the irreversible complex formation (inactivation rate constant).[25] The plot of $1/k_{app}$ against $1/[I]$ yielded a straight line with a positive intercept consistent with the two-step mechanism (Fig. 5B, inset). The values found for K_i and k_{inact} were 260 ± 70 μM and 1.4 ± 0.2 $min,^{-1}$ respectively.

2.3. Molecular modeling study

X-ray crystallographic study has previously performed to explain the enzyme–inhibitor interactions with PTP1B and benzofuran and benzothiophene biphenyls.[26] This work showed that PTP1B has two possible modes of binding at the active site depending on the structures of the ligands. Based on this result, molecular modeling was carried out to study the structural features of the interaction between PTP1B and formylchromone derivatives. FlexX dockings of formylchromones were performed using the Run-Multiple Ligand option of FlexX. The optimal conformational poses of all inhibitors within the active site of the PTP1B and binding orientation of bulk bioactive compounds within the MOLCAD surface area of the X-ray geometry were visually examined (Fig. 6). All the inhibitors were docked into one of the two orientations, which were identified by previous X-ray crystallographic study of the complex of PTP1B and benzothiophene biphenyl derivatives.[26] Detailed binding pattern of an inhibitor **TP34** exhibiting the lowest IC_{50} is shown in Figure 7. In this figure, **TP34** extended deep into the active site pocket, making several

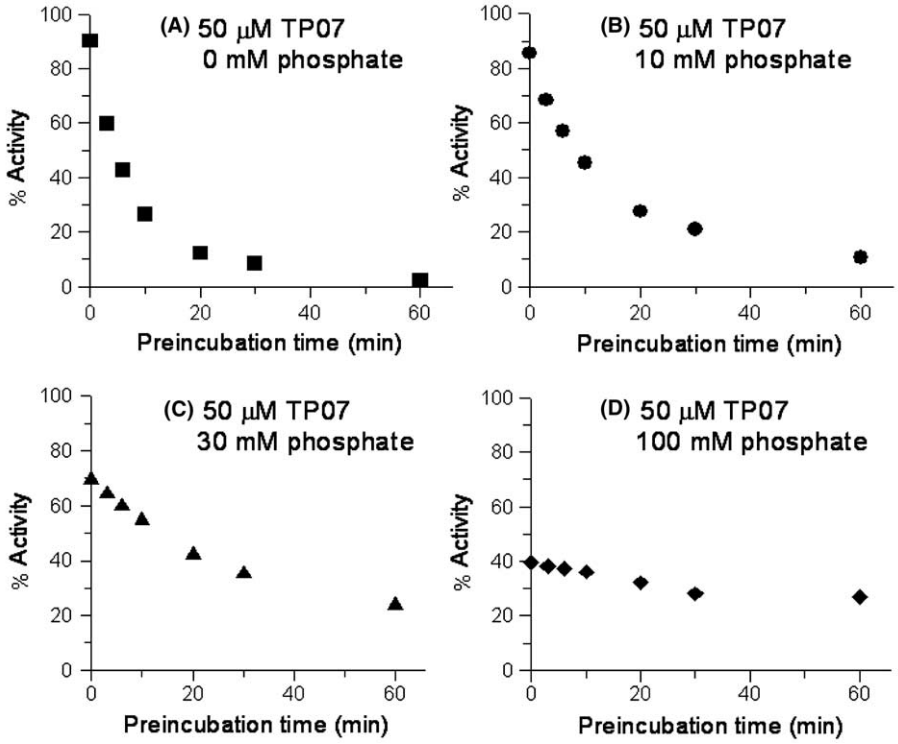

Figure 4. Protective effect of inorganic phosphate against the inactivation of PTP1B by **TP07**. PTP1B was preincubated with **TP07** and inorganic phosphate for the indicated time periods at 25 °C and remaining *p*NPPase activity was measured.

hydrogen bonds and hydrophobic interactions with key residues of the catalytic site. Two carbonyl groups of **TP34** forms three hydrogen bonds with Gly220 and Arg221 and benzopyran group forms van der Waals interaction with phenyl ring of Tyr46 and Phe182.

It is not clear at this stage which amino acid residue of the enzyme forms covalent bond with the inhibitor but modeling study positioned the formyl C atom 3.4 Å away from the S atom of Cys215 and the N atom of Arg221. Formation of S–C bond or N=C bond might be suggested because Cys215 is the catalytic nucleophile and imine formation between Arg221 and cinnamaldehyde derivatives was precedented.[17] In Figure 7, the S atom was oriented perpendicular to the aldehyde carbonyl group facilitating nucleophilic attack to form S–C bond. On the other hand, Arg221 is not oriented in a proper position for imine formation. These observations favor the formation of C–S bond. This issue needs to be further studied.

3. Conclusions

A series of formylchromone derivatives were synthesized and evaluated the inhibitory potency against human PTPases. Most of them inhibited PTPases with different potencies and several of them were potent against PTP1B with IC_{50} values as low as 1.0 μM. They exhibited remarkable selectivity for PTP1B over other human PTPases. The most potent inhibitors, **TP33** and **TP34**, were PTP1B-selective and the IC_{50} values were 500-, 30-, and >10-fold lower than those against LAR-D1, TC-PTP and SHP-1 respectively. Formylchromone moiety is a neutral pharmacophore providing an advantage in drug development in that highly charged inhibitors containing phosphate mimetic might not exhibit good cell permeability. Kinetic studies revealed that formylchromone derivatives are irreversible and active site-directed inhibitors. Molecular modeling study identified the orientation of the inhibitor bound at the active site of PTP1B.

4. Experimental

4.1. Reagents and materials

The substrate for the assay was *p*NPP purchased from Sigma (St. Louis, U.S.A.) as a di(Tris) salt form. Chemicals used for synthesis were from Aldrich (Milwaukee, U.S.A.) or TCI (Tokyo, Japan). Catalytic domain of SHP-1 (SHP-1cat) and His-tagged form of PTP1B were expressed in *E. coli* expression systems and purified as described.[15,27] LAR-D1 (membrane-proximal catalytic domain of LAR) and TC-PTP were purchased from New England Biolabs, Inc. (Beverly, U.S.A.).

4.2. Synthesis of compounds

Formylchromone derivatives used in this study were synthesized from appropriate aryl alcohols using Vilsmeier–Haack reaction as a key step for the construction of the formylchromone skeleton as described in a previous report.[15] General strategy for the synthesis was (i) synthesis of appropriate aryl alcohols, (ii) introduction

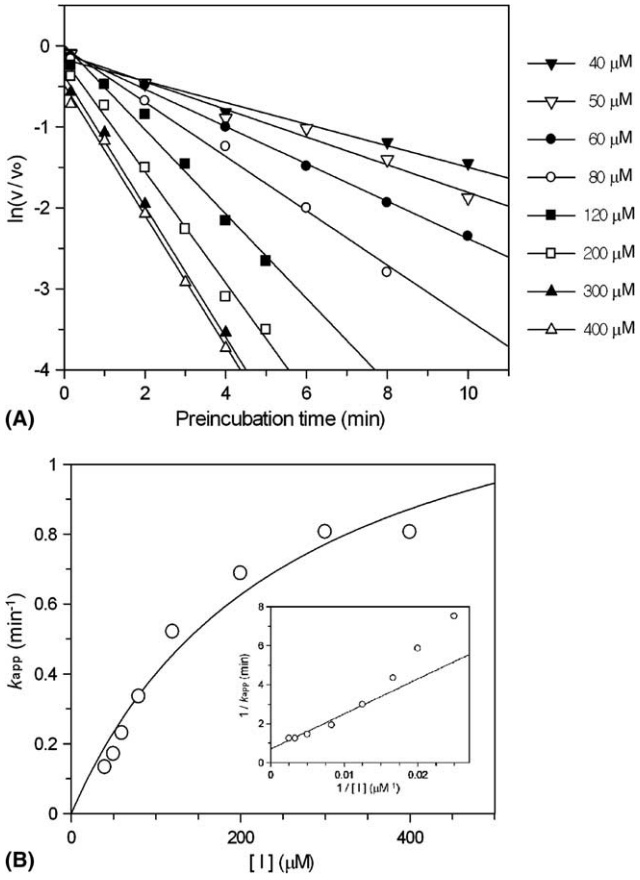

Figure 5. Time and concentration dependent inhibition of PTP1B by **TP07**. (A) To study the kinetics of inactivation, PTP1B was incubated with inhibitor (40–400 μM) at 37 °C in the absence of substrate for given periods of time. Aliquots were taken from the incubated mixture at different time intervals to measure the remaining PTPase activity. The progressive inhibition was plotted as semilogarithmic curve of ln v/v_o versus time. (B) Plot of the first-order inactivation rate (k_{app}) constants for PTP1B versus inhibitor concentrations. (Inset) Double-reciprocal plot of k_{app} versus inhibitor concentrations using GraFit 5.0 program. The curvature-like data points are partly a result of exaggeration of errors during the reciprocal transformation of k_{app} values. Statistical compensation is made for the distorted errors of the data points at low [I] using Lineweaver Burk plot template in GraFit 5.0 program.

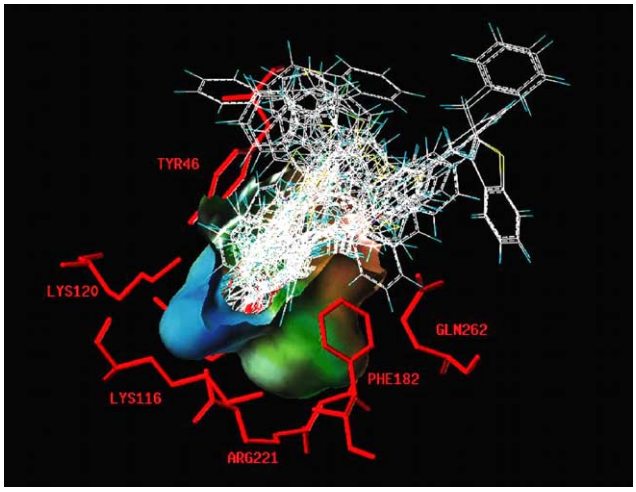

Figure 6. All poses of the binding orientation of formylchromone derivatives at the active site.

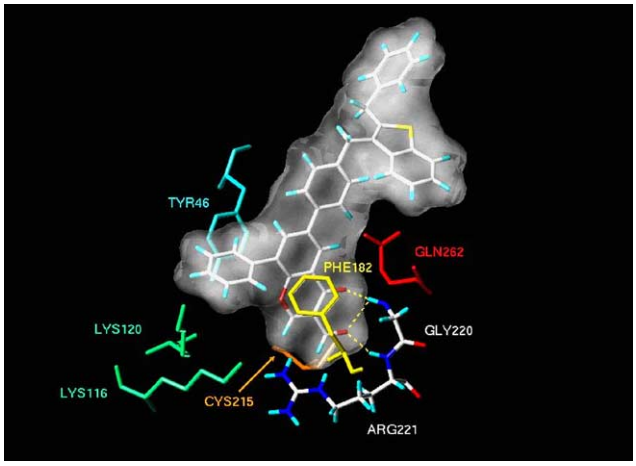

Figure 7. Schematic representation of **TP34** interacting with several key residues of PTP1B within the active site cavity. Sulfur atom of Cys215 is shown as a orange stick.

of acetyl group at the *ortho*-position of the hydroxyl group by Friedel–Crafts acylation, and (iii) reaction of the 2′-hyroxyacetophenone derivatives in the Vilsmeier–Haack condition.

4.3. PTPase assay and determination of IC_{50}

The PTPase activities were determined by measuring the rate of hydrolysis of *p*NPP in buffer A (100 mM Hepes, 5 mM EDTA, pH 7.0). For this assay, the enzyme was diluted with enzyme dilution buffer (25 mM Hepes, 5 mM EDTA, 1 mM DTT, 1 mg/mL bovine serum albumin, pH 7.3) and inhibitors were dissolved in DMSO. Concentration of *p*NPP in the assay mixture was 10 mM unless noted otherwise. The absorbances were measured using Novaspec-II spectrophotometer (Amersham Pharmacia) or DU 650 spectrophotometer (Beckman Coulter). The kinetic data were analyzed using GraFit 5.0 program (Erithacus Software).

For inhibition assay, inhibitor (5 μL) was added to a solution containing enzyme (5 μL), 5× buffer A (10 μL) and H_2O (25 μL) and it was incubated at 37 °C for 10 min before the initiation of the enzyme reaction by addition of *p*NPP solution (5 μL). After 5 min at 37 °C, the enzyme reaction was quenched by addition of 0.5 M NaOH (0.95 mL) and the absorbance at 405 nm was measured to determine the amount of *p*-nitrophenolate released. To determine IC_{50} values, inhibitor solutions of a range of concentrations were added to the assay mixture. The concentrations of PTPases in the assay mixture were 4.7 μg/mL for PTP1B, 22 μg/mL for SHP-1cat, and 25 units (manufacturer's definition)/mL for LAR and TC-PTP IC_{50} values were usually derived from double or triple experiments using a range of inhibitor concentrations.

For continuous assay, enzyme reaction was initiated by addition of 100 μL of diluted PTP1B (1.4 μg/mL final concentration) into a cuvette containing 0.1 mM *p*NPP and various concentrations of inhibitor in buffer A pre-equilibrated to 37 °C and the reaction was continuously monitored at 405 nm by a spectrophotometer equipped with a thermostatic cell holder. The reaction volume was 1 mL and final concentrations of the components were 1.4 μg/mL PTP1B, 0.1 mM *p*NPP, 100 mM Hepes (pH 7.0), 5 mM EDTA, and 0.1 mM DTT (Fig. 2).

For dilution experiment, PTP1B was preincubated for 20 min at 25 °C in the absence or presence of 200 μM **TP07** in enzyme dilution buffer (PTP1B concentration 70 μg/mL). A 12 μL of the mixture was added into the assay solution containing 120 μL of 5× buffer A, 60 μL of 100 mM *p*NPP, and 408 μL of H_2O. Final concentration of the assay mixture was 1.4 μg/mL of PTP1B and 10 mM of *p*NPP. After incubation at 25 °C for a given time periods, a 50 μL aliquot of the mixture was removed and quenched with 950 μL of 0.5 M NaOH solution to measure the absorbance at 405 nm (Fig. 3A). In another experiment, enzyme reaction was initiated by addition of PTP1B (final concentration 1.4 μg/mL) into a cuvette containing 0.1 mM of *p*NPP and 300 μM of **TP07** in buffer A and the absorbances were recorded every 20 s. At 900 s, 10-fold excess *p*NPP was added to the reaction mixture (Fig. 3B).

To examine if inorganic phosphate prevents PTP1B inactivation by formylchromone derivatives, PTP1B was incubated with **TP07** and inorganic phosphate in appropriate concentrations at 25 °C and aliquots were taken at different time points to measure the remaining *p*NPPase activity.

The kinetics of inactivation was studied by incubation of PTP1B (5.0 μg/mL final concentration) with **TP07** (eight concentrations in a range of 40–400 μM) in buffer A in the absence of substrate at 37 °C, pH 7.0. Subsequently, aliquots were taken from the incubated mixture at different time intervals to measure the remaining PTPase activity by addition of *p*NPP to a final concentration of 10 mM. Logarithm of the remaining enzyme activity was plotted against the preincubation time (Fig. 5A). Apparent first-order inactivation rate constants (k_{app}) were calculated from the slope of the lines. To determine the values of K_i and k_{inact}, kinetic analysis were carried out using the method of Kitz and Wilson.[28]

4.4. Molecular modeling

The PTP1B protein structure used in the molecular modeling study was taken from the Protein Data Bank (code name: 1BZJ).[29] Entire 3D structures of diverse ligands were built with Sybyl 6.9 molecular modeling software.[30] All structures were energy minimized by using the Powell method and the standard Tripos force field until an energy gradient of 0.05 kcal mol^{-1} was reached. The atomic charges of all ligands were calculated using the Gasteiger–Hückel method. Even though the minimum energy conformations of the ligands might not be the biologically active conformations, they are a reasonable starting point for comparative purpose and are informative. Low energy conformation was searched by grid search or systematic search method.

Molecular docking between PTP1B and a ligand was performed using the FlexX module[31] implemented in the Sybyl package. FlexX is a fast, flexible directly docking method that uses an incremental construction algorithm to place ligands into an active site. Standard parameters of the FlexX program were used during docking. All the flexibilities of the rotatable bonds of each ligand were considered in the process of docking for identifying the best biding conformation of the ligand with PTP1B. All simulations were performed on IRIX 6.5 Silicon Graphics R10000 workstations. Detailed modeling work will be published elsewhere.

Acknowledgements

This work was supported by the grant (R05-2001-000-00551-0) from the Basic Research Program of the Korea Science & Engineering Foundation. K. C. Kim and S. Shrestha are recipients of BK21 fellowship.

References and notes

1. Zhan, X.-L.; Wishart, M. J.; Guan, K.-L. *Chem. Rev.* **2001**, *101*, 2477.
2. Östman, A.; Böhmer, F. D. *Trends Cell Biol.* **2001**, *11*, 258.
3. Cohen, P. *Trends Biochem. Sci.* **2000**, *25*, 596.
4. Neel, B. G.; Tonks, N. K. *Curr. Opin. Cell Biol.* **1997**, *9*, 193.
5. Zhang, Z.-Y. *Annu. Rev. Pharmacol. Toxicol.* **2002**, *42*, 209.
6. Denu, J. M.; Dixon, J. E. *Curr. Opin. Chem. Biol.* **1998**, *2*, 633.
7. Tonks, N. K.; Diltz, C. D.; Fischer, E. H. *J. Biol. Chem.* **1988**, *263*, 6722.
8. Zhang, Z.-Y. *Curr. Opin. Chem. Biol.* **2001**, *5*, 416.
9. Van Huijsduijnen, R. H.; Bombrun, A.; Swinnen, D. *Drug Discov. Today* **2002**, *7*, 1013.
10. Li, L.; Dixon, J. E. *Semin. Immunol.* **2000**, *12*, 75.
11. Elchebly, M.; Payette, P.; Michaliszyn, E.; Cromlish, W.; Collins, S.; Loy, A. L.; Normandin, D.; Cheng, A.; Himms-Hagen, J.; Chan, C. C.; Ramachandran, C.; Gresser, M. J.; Tremblay, M. L.; Kennedy, B. P. *Science* **1999**, *283*, 1544.
12. Zinker, B. A.; Rondinone, C. M.; Trevillyan, J. M.; Gum, R. J.; Clampit, J. E.; Waring, J. F.; Xie, N.; Wilcox, D.; Jacobson, P.; Frost, L.; Kroeger, P. E.; Reilly, R. M.; Koterski, S.; Opgenorth, T. J.; Ulrich, R. G.; Crosby, S.; Butler, M.; Murray, S. F.; McKay, R. A.; Bhanot, S.; Monia, B. P.; Jirousek, M. R. *Proc. Natl. Acad. Sci. U.S.A.* **2002**, *99*, 11357.
13. Rondinone, C. M.; Trevillyan, J. M.; Clampit, J.; Gum, R. J.; Berg, C.; Kroeger, P.; Frost, L.; Zinker, B. A.; Reilly, R.; Ulrich, R.; Butler, M.; Monia, B. P.; Jirousek, M. R.; Waring, J. F. *Diabetes* **2002**, *51*, 2405.
14. Ramachandran, C.; Kennedy, B. P. *Curr. Top. Med. Chem.* **2003**, *3*, 749.
15. Shim, Y. A.; Kim, K. C.; Chi, D. Y.; Lee, K.-H.; Cho, H. *Bioorg. Med. Chem. Lett.* **2003**, *13*, 2561, and references cited therein.

16. Taylor, S. D. *Curr. Top. Med. Chem.* **2003**, *3*, 759.
17. Fu, H.; Park, J.; Pei, D. *Biochemistry* **2002**, *41*, 10700.
18. Liljebris, C.; Martinsson, J.; Tedenborg, L.; Williams, M.; Barker, E.; Duffy, J. E. S.; Nygren, A.; James, S. *Bioorg. Med. Chem.* **2002**, *10*, 3197.
19. Wipf, P.; Aslan, D. C.; Southwick, E. C.; Lazo, J. S. *Bioorg. Med. Chem. Lett.* **2001**, *11*, 313.
20. Malamas, M. S.; Sredy, J.; Gunawan, I.; Mihan, B.; Sawicki, D. R.; Seestaller, L.; Sullivan, D.; Flam, B. R. *J. Med. Chem.* **2000**, *43*, 995.
21. Watanabe, T.; Suzuki, T.; Umezawa, Y.; Takeuchi, T.; Otsuka, M.; Umezawa, K. *Tetrahedron* **2000**, *56*, 741.
22. Ham, S. W.; Park, J.; Lee, S.-J.; Yoo, J. S. *Bioorg. Med. Chem. Lett.* **1999**, *9*, 185.
23. Huang, P.; Ramphal, J.; Wei, J.; Liang, C.; Jallal, B.; McMahon, G.; Tang, C. *Bioorg. Med. Chem.* **2003**, *11*, 1835.
24. Cho, H.; Lee, D. Y.; Shrestha, S.; Shim, Y. S.; Kim, K. C.; Kim, M.-K.; Lee, K.-H.; Won, J.; Kang, J.-S. *Mol. Cells* **2004**, *18*, 46.
25. Dinos, G. P.; Coutsogeorgopoulos, T. L. C. *J. Enzyme Inhib.* **1997**, *12*, 79.
26. Malamas, M. S.; Sredy, J.; Moxham, C.; Katz, A.; Xu, W.; McDevitt, R.; Adebayo, F. O.; Sawicki, D. R.; Seestaller, L.; Sullivan, D.; Taylor, J. R. *J. Med. Chem.* **2000**, *43*, 1293.
27. Pei, D.; Neel, B. G.; Walsh, C. T. *Proc. Natl. Acad. Sci. U.S.A.* **1993**, *90*, 1092.
28. Kitz, R.; Wilson, I. B. *J. Biol. Chem.* **1962**, *237*, 3245.
29. Berman, H. M.; Westbrook, J.; Feng, Z.; Gilliland, G.; Bhat, T. N.; Weissig, H.; Shindyalov, I. N.; Bourne, P. E. *Nucleic Acids Res.* **2000**, *28*, 235.
30. Sybyl 6.9, Tripos Inc., 1699 South Hanley Rd., St. Louis, MO 63144, USA.
31. Rarey, M.; Kramer, B.; Lengauer, T.; Klebe, G. *J. Mol. Biol.* **1996**, *261*, 470.